

## Flotation efficiency of activated sludge flocs using population balance model in dissolved air flotation

Heung-Joe Jung, Jae-Wook Lee, Do-Young Choi, Seong-Jin Kim\* and Dong-Heui Kwak<sup>†</sup>

Department of Environment and Chemical Engineering, Seonam University, Gwangchi Dong, Namwon, Jeonbuk 590-711, Korea

\*Department of Sanitary and Environmental, Hanyeong College, Yeosu, Jeonnam 550-260, Korea

(Received 7 July 2005 • accepted 26 October 2005)

**Abstract**—The activated sludge process is one of the most frequently used processes for biological wastewater treatment. Conventional gravity sedimentation (CGS), which is widely used as a secondary clarifier in activated sludge processes, has a routine problem due to floating tendency, called bulking, caused by filamentous microorganisms. Dissolved air flotation (DAF) has been applied as potential alternative to CGS as a secondary clarifier. A series of experiments were performed to measure physico-chemical characteristics and removal efficiency of activated sludge flocs. The removal efficiency of flocs corresponding in lag and exponential growth phases was lower, while that of flocs both in stationary and endogenous phases considerably increased. The rise velocity of floc/bubble agglomerates was calculated by using a population balance (PB) model explaining the distribution of floc/bubble agglomerates. The experimental results of flotation efficiency showed a similar tendency with the results predicted by PB model for the rise velocity and distribution of floc/bubble agglomerates. It was found from our study that the DAF process was very effective as a secondary clarifier in the activated sludge process.

Key words: DAF, Dissolved Air Flotation, Population Balance Model, Activated Sludge, Flotation Efficiency

### INTRODUCTION

The activated sludge process, which is one of the most frequently used processes for biological wastewater treatment, consists of two stages, a biochemical stage (aeration tank) and a physical stage (secondary clarifier). In the aeration tank, organic carbon, ammonium and phosphate are removed from the wastewater by the activated sludge. The diversity of the biological community is very large, containing many species of bacteria, protozoa, fungi, metazoa and algae. In the secondary clarifier, gravity sedimentation has been widely used as solid separation of biological flocs or sludge in wastewater treatment [Lee and Hano, 2001]. However, the sedimentation process has a routine problem due to floating tendency, called bulking, caused by filamentous microorganisms [Martins et al., 2004]. Bulking sludge, a term used to describe the excessive growth of filamentous bacteria, is a common problem in the activated sludge process.

Dissolved air flotation (DAF) is a method of water treatment that historically has been used primarily for sludge thickening. This process has started to gain wide acceptance for algae-contained, low-turbidity, low-alkalinity or colored waters that produce low density flocs [Zabel, 1985]. Moreover, DAF has been effectively used in the treatment of municipal and industrial wastewater containing high suspended solids concentration [Kwak et al., 2005; Lee et al., 2005]. Therefore, the DAF process has been applied as a potential alternative to the conventional gravity sedimentation (CGS) process as a secondary clarifier in the activated sludge process. Also, the DAF process should be used to solve the problem of bulking effectively.

The leading DAF models reported in literature are classified into

two groups. The first model is the single-collector collision (SCC) model [Edzwald et al., 1991]. This model treats each bubble as a single collector of particles under laminar conditions and considers all the bubbles as a 'white water' blanket. The second model is the population balance in turbulence (PBT) model [Fukushi et al., 1995]. The PBT approach describes collisions between bubbles and particles through kinetic expression using a population balance. Both models divide a DAF unit into two zones: contact (reaction) and separation. The contact zone encourages attachment between bubbles and particles or flocs, while the separation zone promotes clarification as bubble/floc agglomerate float to the surface. In this paper, only the second model will be used as an aid to understanding the DAF process as a clarifier in the activated sludge process. Leppinen [2001] has proposed a kinetic model modifying that of Fukushi et al. [1995] in order to predict the rise velocity of bubble/floc agglomerates during flotation. This rise velocity was dependent on a number of factors including the bubble size, the particle or floc size, the density of bubble and flocs, the viscosity of water, the number of bubbles attached on floc and the residence time of fluid within the contact zone. If the number of attached bubbles on floc increases, the rise velocity of the bubble/floc agglomerate increases. Unfortunately, studies on the application of DAF process for activated sludge treatment have been very limited so far.

This paper focused on the measurement of physico-chemical characteristics (i.e., MLSS concentration and COD) and floating tendency of activated sludge flocs in the DAF process. The extended PB model considering the entire range of Reynolds number ( $N_{Re}$ ) and temperature effect was proposed to evaluate the experimental flotation efficiency of activated sludge flocs. In addition, the feasibility of the DAF process as a secondary clarifier for activated sludge treatment was reviewed under various operating conditions.

\*To whom correspondence should be addressed.

E-mail: kwak124@seonam.ac.kr

## THEORETICAL APPROACH

### 1. Rise Velocity of Bubble/Floc Agglomerate

The diameter of bubble/floc agglomerate ( $d_{aggom}$ ) and the density of bubble/floc agglomerate ( $\rho_{aggom}$ ) composing one particle (or floc) and i-bubbles are calculated by using Eqs. (1) and (2).

$$d_{aggom} = (d_p^3 + d_b^3)^{1/3} \quad (1)$$

$$\rho_{aggom} = \frac{\rho_p d_p^3 + i \rho_b d_b^3}{d_p^3 + i d_b^3} \quad (2)$$

In this study, three variables, water density,  $\rho$ , water viscosity,  $\mu$  and density of air bubble,  $\rho_b$ , are represented as functions of temperature. In particular,  $\mu$  and  $\rho_b$  are strongly dependent upon temperature. The water density [Vlyssides et al., 1986] can be written as:

$$\rho = 1006.63 e^{-0.00014(1.8(T-273.15)+32)} \quad (3)$$

The viscosity of water [Reid et al., 1987] can be approximated as:

$$\ln \mu = A + B/T + C/T^2 + D/T^3 \quad (4)$$

The density of air bubbles in the contact zone can be calculated by Eq. (5)

$$\rho_b = \frac{M_{w,air}(P_{atm} + \rho g h_m)}{RT} \quad (5)$$

where  $h_m$  is the height of contact zone. The total buoyancy force acting on bubble/floc agglomerates is represented as follows:

$$F_{Buoyancy} = \frac{\pi d_{aggom}^3 (\rho - \rho_{aggom}) g}{6} \quad (6)$$

where  $g$  is the gravity acceleration. The Reynolds number of agglomerates is calculated by

$$N_{Re} = \frac{\rho v_i d_{aggom}}{\mu} \quad (7)$$

where  $v_i$  is the velocity of agglomerate which attach i-bubbles on the floc. The drag force,  $F_{Drag}$ , acting on bubble/floc agglomerates can readily be calculated as a function of its velocity through known correlations of sphere's drag coefficient,  $C_D$ , as function of  $N_{Re}$  as follows:

$$C_D = \frac{F_{Drag}}{\pi \rho v_i^2 d_{aggom}^2 / 8} \quad (8)$$

With the substitution of  $F_{Buoyancy} = F_{Drag}$  into Eq. (8), the rise velocity of the agglomerates can be written as:

$$v_i = \left( \frac{F_{Buoyancy}}{C_D \pi \rho d_{aggom}^2 / 8} \right)^{1/2} \quad (9)$$

The drag coefficient correlation in sphere recommended by Clift et al. [1978] is represented by the function of Reynolds number,  $N_{Re}$ , divided into four intervals as follows:

$$C_D = \begin{cases} \frac{24}{N_{Re}} \left( 1 + \frac{3}{16} N_{Re} \right) & N_{Re} < 0.01 \\ \frac{24}{N_{Re}} \left( 1 + 0.1315 N_{Re}^{0.82 - 0.05 \log_{10} N_{Re}} \right) & 0.01 \leq N_{Re} < 20 \\ \frac{24}{N_{Re}} \left( 1 + 0.1935 N_{Re}^{0.6305} \right) & 20 \leq N_{Re} < 260 \\ 10^{1.6435 - 1.1242 \log_{10} N_{Re} + 0.1558 (\log_{10} N_{Re})^2} & 260 \leq N_{Re} \leq 1.5 \times 10^3 \end{cases} \quad (10)$$

Contrary to Leppinen et al. [2001], we have expressed the drag coefficient with entire range of  $N_{Re}$  covering including laminar and transient region in this work. The rise velocity of the agglomerates is determined by solving Eqs. (7) to (10) using a least square method known as the Levenberg-Marquardt algorithm as an initial trial value with Stokes approximation represented by Eq. (11):

$$v_{i,cr} = \frac{(\rho - \rho_{aggom}) g d_{aggom}^2}{18 \mu} \quad (11)$$

which corresponds to the limit of  $N_{Re} \rightarrow 0$ .

The maximum number of attached bubbles on a floc suggested by Matsui et al. [1998] can be written as:

$$i_{max} = \max(1, c(d_p/d_b)^2) \quad (12)$$

where  $[x]$  is the largest integer and  $c$  is a numeric constant. We will be using the empirical value,  $c=1$ , suggested by Matsui et al. [1998] in this study.

### 2. Population Balance Model in Contact Zone

A population balance describing the process of bubble-floc collision and attachment was formulated by counting the number of flocs attached i-bubbles,  $n_i$ , at mixing time,  $t$ . On the basis of the of assumptions reported by Fukushi et al. [1995] and modified by Leppinen et al. [2001], the number of flocs attached i-bubbles,  $n_i$ , represented by the ordinary differential equations as follows:

$$\frac{dn_0}{dt} = -k \alpha_0 n_0 n_{bubbles} \quad (13)$$

$$\frac{dn_i}{dt} = k \alpha_{i-1} n_{i-1} n_{bubbles} - k \alpha_i n_i n_{bubbles}, \quad i = 1 \text{ to } i_{max} \quad (14)$$

where  $k$  is the turbulent collision rate constant represented by following equation.

$$k = aG(d_p + d_b)^3 \quad (15)$$

And  $n_{bubbles}$  is the number of bubbles per unit volume in contact zone described as:

$$n_{bubbles} = \frac{\phi}{\pi d_b^3 / 6} \quad (16)$$

Adhesion efficiency ( $\alpha$ ) determined by the ratio of size of between bubble and floc and the number of attached bubbles can be written as:

$$\alpha_i = \begin{cases} \alpha_0 \left( 1 - \frac{d_b^3}{d_p^3} \right), & i = 1 \text{ to } i_{max} - 1 \\ 0, & i = i_{max} \end{cases} \quad (17)$$

With the substitution of Eqs. (15) to (17) into Eqs. (13) to (14), the differential equations can be written as:

$$\frac{dn_0}{dt} = -aG(d_p + d_b)^3 \frac{\phi}{\pi d_b^3 / 6} \alpha_0 n_0 \quad (18)$$

$$\frac{dn_i}{dt} = aG(d_p + d_b)^3 \frac{\phi}{\pi d_b^3 / 6} \left( \left( 1 - (i-1) \frac{d_b^3}{d_p^3} \right) n_{i-1} - \left( 1 - i \frac{d_b^3}{d_p^3} \right) n_i \right), \quad i = 1 \text{ to } i_{max} - 1 \quad (19)$$

$$\frac{dn_{i_{max}}}{dt} = aG(d_p + d_b)^3 \frac{\phi}{\pi d_b^3 / 6} \left( 1 - (i_{max} - 1) \frac{d_b^3}{d_p^3} \right) n_{i_{max} - 1} \quad (20)$$

Eqs. (18) to (20) are solved subject to the initial conditions  $n_0 = N_0$  and  $n_i = 0$  for all  $i \geq 1$ , when  $t=0$  in order to determine the values of  $n_i$  after a retention time of  $t=t_{contact}$  in the contact zone. Introducing the dimensionless variables  $t^* = t/t_{contact}$  and  $n_i^* = n_i/N_0$ , Eqs. (18) to (20) can be represented for dimensionless form as:

$$\frac{dn_0^*}{dt^*} = -\kappa n_0^* \quad (21)$$

$$\frac{dn_i^*}{dt^*} = \kappa \left( \left( 1 - (i-1) \frac{d_p^2}{d_b^2} \right) n_{i-1}^* - \left( 1 - i \frac{d_p^2}{d_b^2} \right) n_i^* \right), \quad i = 1 \text{ to } i_{max} - 1 \quad (22)$$

$$\frac{dn_{i_{max}}^*}{dt^*} = \kappa \left( 1 - (i_{max} - 1) \frac{d_p^2}{d_b^2} \right) n_{i_{max}-1}^* \quad (23)$$

Dimensionless flotation rate constant,  $\kappa$ , can be represented as:

$$\kappa = \frac{6aGt_{contact} \left( 1 + \frac{d_p}{d_b} \right)^3 \phi \alpha_0}{\pi} \quad (24)$$

Applying Laplace transformation, the number of flocs attached with  $i$  bubbles can be represented as:

$$n_i^* = \binom{d_p^2/d_b^2}{i} \exp(-\kappa t^*) \left( \exp\left(\frac{\kappa t^*}{d_p^2/d_b^2}\right) - 1 \right) \quad i = 0 \text{ to } i_{max} - 1 \quad (25)$$

$$n_{i_{max}}^* = 1 - \sum_{i=0}^{i_{max}-1} n_i^* \quad (26)$$

where the generalized combinational is defined as Eq (27):

$$\binom{x}{i} = \frac{x!}{i!(x-i)!} = \frac{x(x-1)A(x-(i-1))}{i(i-1)A(2)(1)} \quad (27)$$

### 3. Flotation Efficiency in the Contact Zone

The overall efficiency of a DAF tank is determined by relating the rise velocity of bubble/floc agglomerates leaving the contact zone to the surface loading rate of the tank. If the the rise velocity of bubble/floc agglomerates is  $v_r$ , and the surface loading rate is  $v_{SL}$ , then overflow theory [Matsui et al., 1998] can be used to calculate the removal fraction,  $\eta$ , written as:

$$\eta = \min(1, \max(0, v_r/v_{SL})) \quad (28)$$

where  $\eta$  represents the fraction of bubble/floc agglomerates which exit to the contact zone.

The flotation efficiency of the DAF is modeled by combining the results for the rise velocities of bubble/floc agglomerates with the results from the population balance model in order to predict the distribution of the rise velocities of the bubble/floc agglomerates as they leave the contact zone of the DAF tank. Summing overall bubble/floc agglomerates and combining Eqs. (25), (26) and (28), the flotation efficiency can be written as:

$$\eta = \sum_{i=0}^{i_{max}} n_i^* (t^* = 1) \cdot \eta_i = \sum_{i=0}^{i_{max}} n_i^* (t^* = 1) \min(1, \max(0, v_r/v_{SL})) \quad (29)$$

## MATERIALS AND METHODS

### 1. Experimental Set-up and Operation

Activated sludge was cultured in a batch reactor as shown Fig. 1. The batch reactor was 20 L in volume and manufactured by acryl.

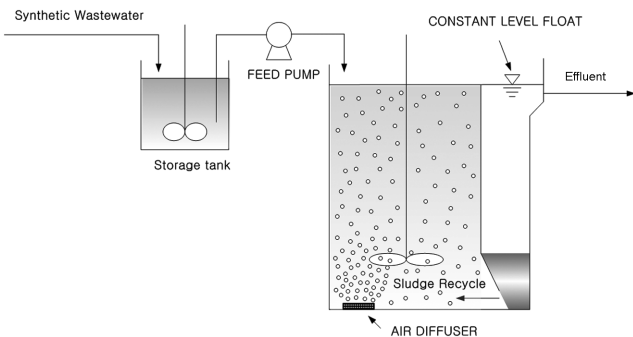


Fig. 1. Schematic diagram of the activated sludge reactor.

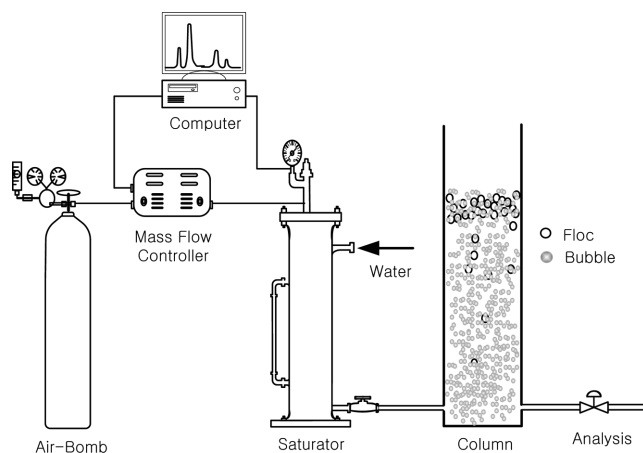


Fig. 2. Schematic diagram of batch-type DAF equipment.

The reactor was composed of wastewater storage tank, activated sludge tank and settling tank. Synthetic wastewater was prepared similar to general domestic wastewater. The composition of the synthetic wastewater was as follows: dextrose, 450 mg/l;  $\text{NH}_4\text{Cl}$ , 120 mg/l,  $\text{K}_2\text{HPO}_4$ , 70 mg/l;  $\text{Na}_2\text{CO}_3$ , 420 mg/l; KCl, 80 mg/l;  $\text{CuCl}_2$ , 40 mg/l, NaCl, 80 mg/l,  $\text{MgSO}_4$ , 40 mg/l and trace element solution, 1.0 mL/l. The values of BOD, COD and MLSS were measured by APHA-AWWA-WPCF standard methods for the examination of water and wastewater [APHA-AWWA-WPCF standard method, 1998].

The seed microorganisms, activated sludge from domestic wastewater treatment plant in N city, Korea, were domesticated during three weeks in an activated sludge reactor, cultured and sampled for water quality test.

A schematic diagram of the DAF apparatus is shown in Fig. 2. The diameter of the flotation column made of Plexiglas was 0.15 m, and the height was 1.8 m. Activated sludge flocs were suspended initially in the column, then bubbles were introduced in the column from the bottom side of the column. The dissolved air solution was fed into the flotation column for 4 min and the particles in the column were removed by the rising bubbles. The mean diameter of the bubbles fed into the column was 30  $\mu\text{m}$ . After all the bubbles in the cell reached the top of the column, the solution was sampled to obtain the flotation efficiency. The turbidity was measured by using the turbidity meter (HACH 2100P). The floc and bubble sizes were measured with a particle size analyzer (model No. PC2400D, Chemtrac Co., USA).

## RESULTS AND DISCUSSION

### 1. Growth of Microbial Biomass

The physico-chemical characteristics, such as COD and MLSS concentration, were measured in an activated sludge reactor. Substrate concentration was decreased from initial feed concentration 144 mg/L to 23 mg/L in COD during three days. The value of consumption was 121 mg/L (i.e. 84% consumption for initial concentration). In addition, the growth rate of microbial biomass was investigated in terms of cultured time. As shown in Fig. 3, MLSS concentration shaped S curve is the indicator for the microbial growth. From the experimental results of MLSS concentration, there are four phases, such as lag, exponential, stationary and endogenous state [Lee, 1992]. The lag phase is an initial period of cultivation during which the change of cell number is negligible. Even though the cell number does not increase, the cells may grow in size during this period. At the end of the lag phase, when growth begins, the division rate increases gradually and the maximum value is in the exponential growth period. The growth of microbial population is normally limited either by the exhaustion of available nutrients or by the accumulation of toxic products of metabolism. As a consequence, the rate of growth declines and growth eventually stops. At this point a culture is in the stationary phase. The stationary phase is followed by a death phase, so-called endogenous phase, in which the organisms die. Death occurs either because of the depletion of the cellular reserves of energy, or the accumulation of toxic products.

Flotation efficiency is affected by floc size. Thus, the average diameter of floc is measured to apply to PB model in the DAF process. Fig. 4 shows the diameter variation of the average flocs. The results describe that the diameter is increased in the lag and exponential growth phases, while the same size is maintained after the stationary phase.

### 2. Flotation and Sedimentation Efficiencies

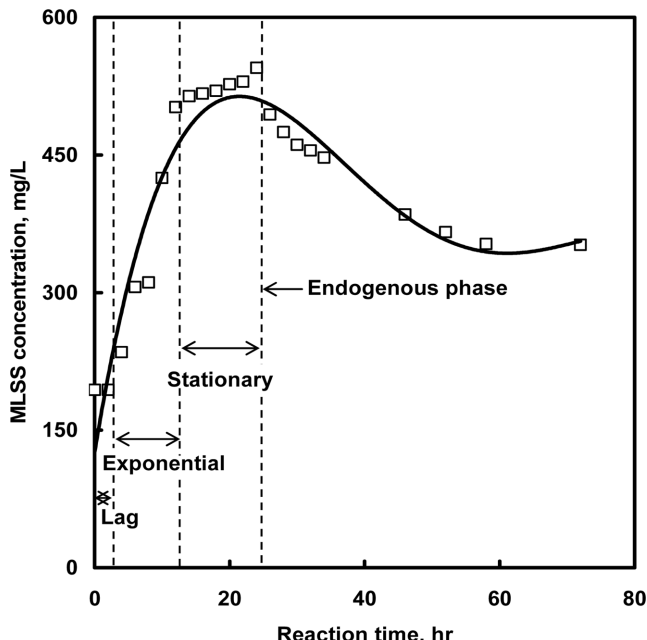


Fig. 3. Variation of MLSS concentration for growth time of microbial biomass.

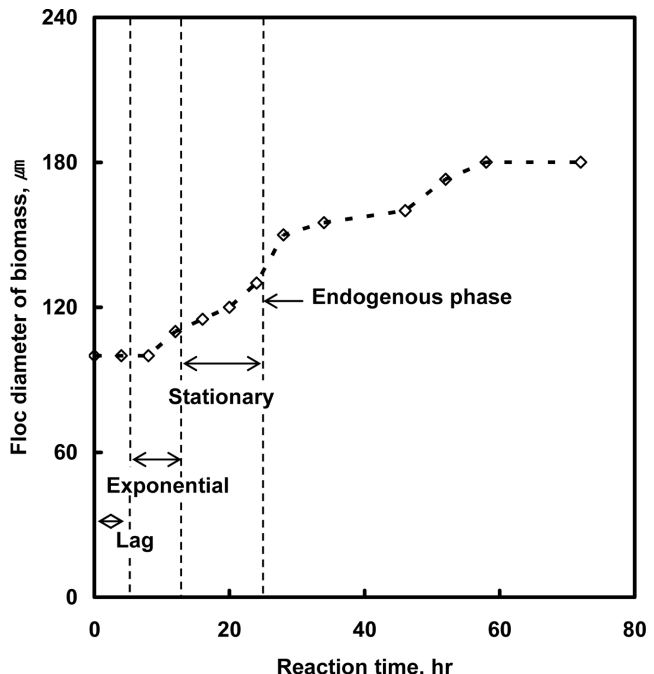


Fig. 4. Variation of floc size for growth time of microbial biomass.

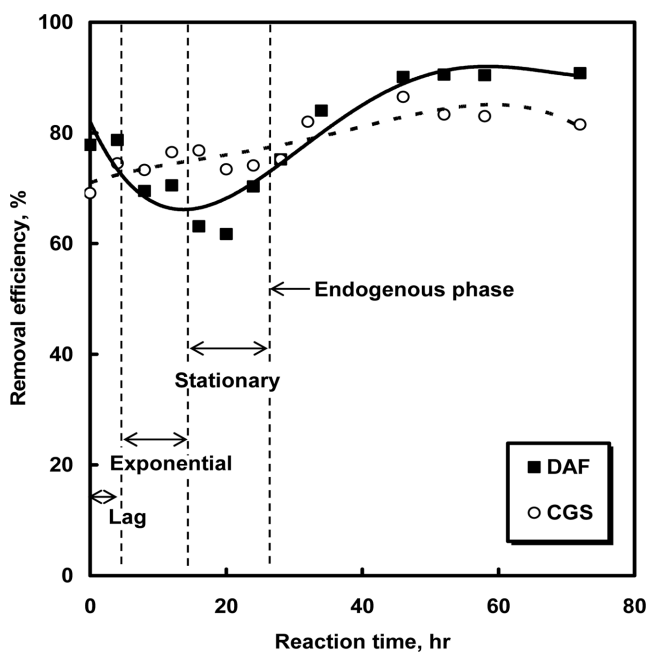


Fig. 5. Comparison of removal efficiency between DAF and CGS processes in terms of growth time.

As shown in Fig. 5, flotation efficiency varied according to the growth state. Flotation efficiency rapidly decreased from lag phase to exponential phase, while gradually increasing in stationary and endogenous phases. In addition, sedimentation efficiency was observed for comparison purpose. Here, the sample used was obtained after settling 30 min from the flotation column. Both sedimentation and flotation gave similar efficiencies. Flotation efficiency was lower for the exponential growth phase, while it was relatively higher for the stationary phase. This resulted from the fact that the growth state

of biomass highly depends on the initial adhesion efficiency, floc density, and the concentration and the size of floc etc.

One of advantages of the DAF process for activated sludge wastewater treatment is that it can be operated within a very short time (i.e., 2-4 min) compared to CGS (more or less 30 min). The amount of consuming air bubbles per mass of floc in DAF is generally 0.25 mg air/mg floc.

### 3. Estimation of Initial Adhesion Efficiency ( $\alpha_0$ ) for Biomass Flocs

Initial adhesion efficiency ( $\alpha_0$ ) means the collision-attachment affinity between floc and bubble. In this work, initial adhesion efficiency of the biomass is estimated by using the method suggested by Matsui et al. [1998]. Fig. 6 illustrates that the correlation of the distribution of floc with i-attached bubble and the rise velocity of the bubble/floc agglomerate. The solid lines are the predicted results. The initial adhesion efficiency ( $\alpha_0$ ) between bubble and floc was

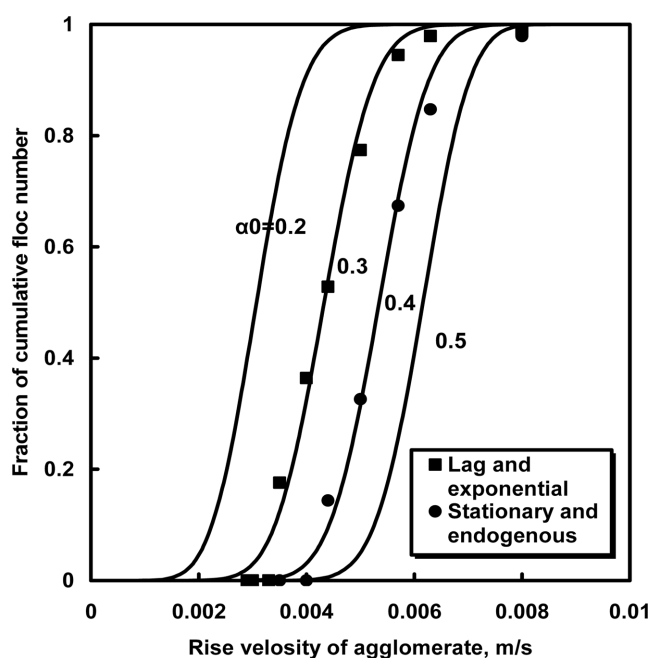


Fig. 6. Estimation of the initial adhesion efficiency ( $\alpha_0$ ) using PB model.

Table 1. Parameters using population balance model in DAF process

Parameters	Value	Unit	Reference
Diameter of bubble ( $d_b$ )	$3.0 \times 10^{-5}$	m	
Diameter of floc ( $d_p$ )	$1.0-5.0 \times 10^{-4}$	m	
Density of water ( $\rho$ ) at 293.15 K	$1.0 \times 10^3$	kg/m <sup>3</sup>	
Density of bubble ( $\rho_b$ ) at 293.15 K	$1.17 \times 10^{-3}$	kg/m <sup>3</sup>	Liers et al. [1996]
Viscosity of water ( $\mu$ ) at 293.15 K	$1.306 \times 10^{-2}$	kg/m·s	Reid et al. [1987]
Temperature of water (T)	293.15	K	
Numerical constant (a)	$5.0 \times 10^4$	-	Saffman and Turner [1956]
Turbulent dissipation of energy ( $\epsilon_0$ )	$6.0 \times 10^{-3}$	W/m <sup>3</sup>	
Bubble volume concentration ( $\phi$ )	0.0046	m <sup>3</sup> /m <sup>3</sup>	Edzwald [1995]
Turbulent intensity (G)	10	s <sup>-1</sup>	
Initial adhesion efficiency ( $\alpha_0$ )	0.3 or 0.4	-	
Surface loading rate ( $v_{SL}$ )	0.0015	m/s	

roughly 0.3 for exponential phase and roughly 0.4 for endogenous phase. On the basis of this result, one should be very careful to choose the initial adhesion efficiency ( $\alpha_0$ ) of biomass according to the growth phase in the design of the DAF process.

### 4. Rise Velocity of Bubble/Floc Agglomerates in PB Model

By using Eq. (1) to Eq. (11) the maximum rise velocity of the bubble/floc agglomerate can be predicted as functions of the bubble and floc sizes. The model parameters of extended PB model are listed in Table 1. Maximum rise velocity represented the velocity of agglomerates which attached possible maximum number of bubbles upon one floc by Eq. (12). Fig. 7 shows the maximum rise velocity in terms of floc size. The maximum number of bubbles attached on the floc (Eq. (12)) for bubble diameters ( $d_b=20, 25, 30, 35$  and  $40 \mu\text{m}$ ) was calculated by solving Eqs. (7) to (10) using the least square method known as the Levenberg-Marquardt algorithm.

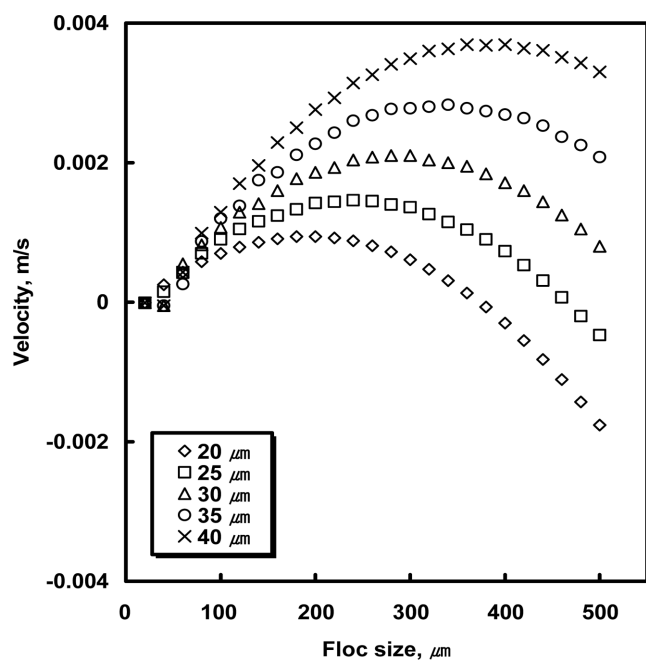


Fig. 7. Maximum rise velocity of bubble/floc agglomerates as a function of floc size for bubble diameter  $d_b=20, 25, 30, 35$  and  $40 \mu\text{m}$ .

As the number of bubbles increases, the rise velocity of the bubble/floc agglomerates increases. A positive sign of the maximum rise velocity represents the flotation of agglomerates, while a negative sign denotes the sedimentation of agglomerates. The global maximum rise velocity for each size of bubble can be observed. As the bubble diameter increases, the global maximum rise velocity increases. In addition, the highest value of the maximum rise velocity moves to higher floc size as increasing the bubble size. Although the maximum rise velocity does not mean the real DAF process, the results imply an upper limitation of the rise velocity.

### 5. Model Parameter Sensitivity

Eqs. (1) to (11) show that the flotation efficiency is a function of the initial adhesion efficiency, the diameter of particle or floc, the bubble diameter, the surface loading rate, the bubble volume concentration, the temperature and the residence time in the contact zone. In several works of bubble size distribution [Rodrigues and Rubio, 2003; Lee et al., 2003; Vlyssides et al., 2004; Leppinen and Dalziel, 2004], the mean diameter of bubble size was suggested as being from 25 to 100  $\mu\text{m}$ . In preliminary work, the bubble size was measured to about 30  $\mu\text{m}$  [Lee et al., 2005].

Fig. 8 illustrates the influence of the initial adhesion efficiency as a function of floc size under the condition of  $d_b=30 \mu\text{m}$ . The initial adhesion efficiency is varied from 0.2 to 0.6 because many studies [Fukushi et al., 1995; Liers et al., 1996; Leppinen et al., 2001] mentioned that the initial adhesion efficiency is in the range 0.1-1.0, and in most practical cases ranges from 0.3 to 0.4. Fig. 8 shows that too low initial adhesion efficiency values give low flotation efficiency. However, in the range of 0.3-0.6, the predicted efficiencies are  $>90\%$  in the floc larger than  $d_f=150 \mu\text{m}$ .

Fig. 9 illustrates the sensitivity of the model for the surface loading rate,  $v_{SL}$ , which means the linear rate of liquid flow in the contact zone. For analysis, the parameter is varied from 0.005 m/s to 0.075 m/s. For low surface loading rates (i.e., 0.005 and 0.015 m/s), the

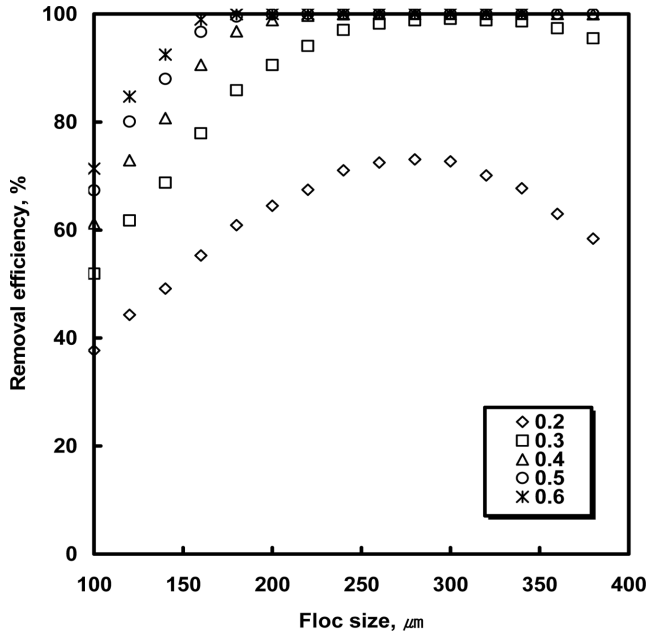


Fig. 8. Influence of the initial adhesion efficiency ( $\alpha_0$ ) as a function of floc size on the flotation efficiency size in the contact zone.

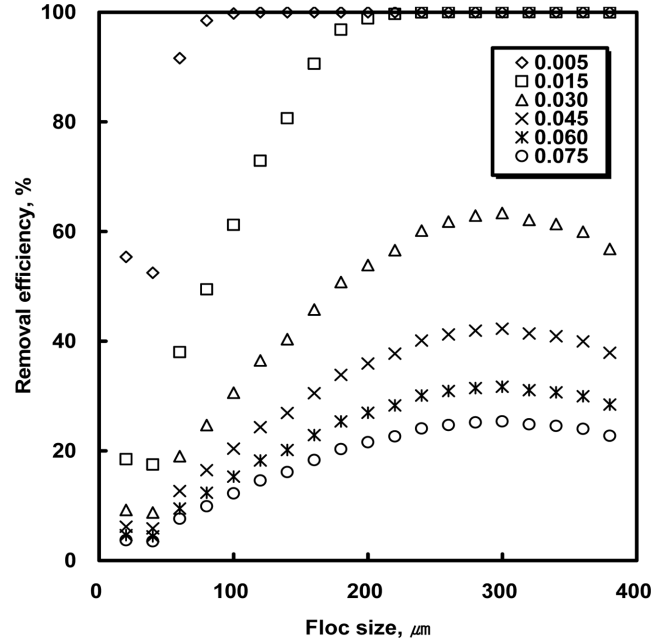


Fig. 9. Influence of the surface loading rate ( $v_{SL}$ ) as a function of floc size on the flotation efficiency.

flotation efficiency approaches 100%. But the flotation efficiency was very low for high surface loading rate. This indicates that the model is very sensitive to this parameter. This is very important: the longer the contact time is, the higher flotation efficiency achieved.

The flotation efficiency is a function of temperature because the viscosity of water and density of bubbles and water are dependent on the temperature. Fig. 10 illustrates the influence of the temperature on the flotation efficiency. This result indicates that higher temperature will give higher efficiencies. Using model parameters given

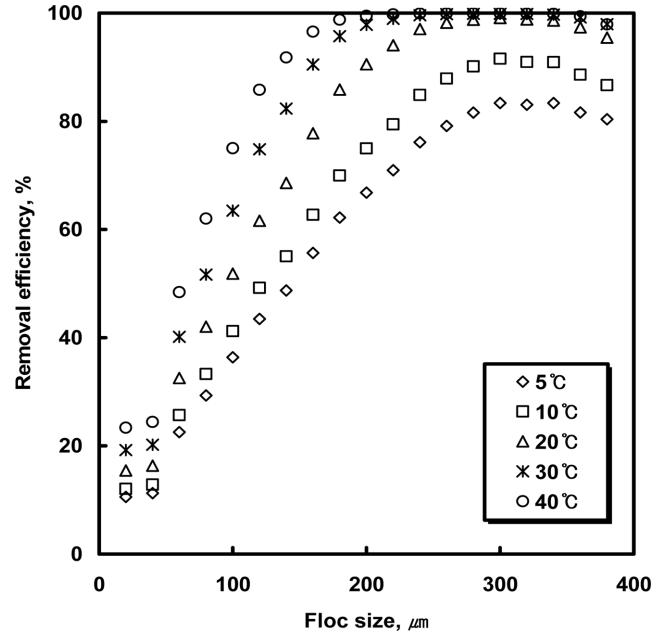


Fig. 10. Influence of the operating temperature on the flotation efficiency as a function of floc size in the contact zone.

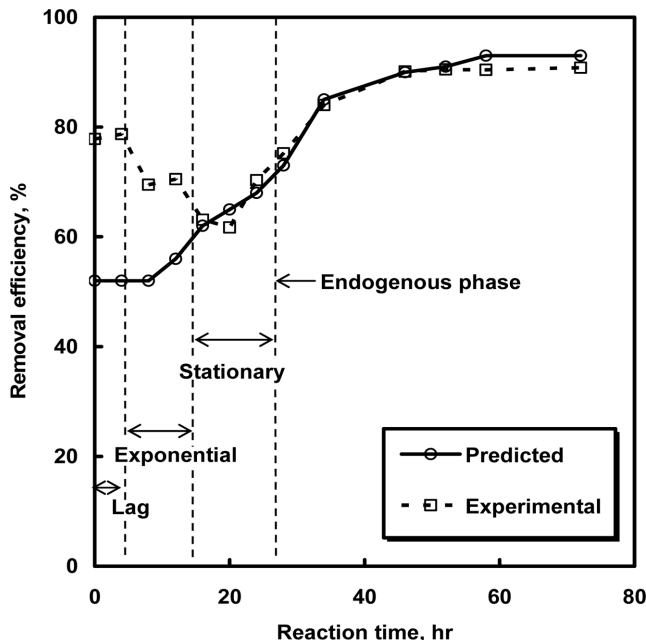


Fig. 11. Comparison of removal efficiency of experimental and predicted results using population balance model.

Table 1, the model predicted that a difference of 10 °C will give a difference of 10% in efficiency.

#### 6. Flotation Efficiency Estimation

Fig. 11 illustrates the experimental and predicted flotation efficiencies. For this calculation, we use just 0.3 for the exponential growth phase and 0.4 for stationary and endogenous phases. A slight difference between experimental and predicted results can be observed at below 20 h. Thereafter, good agreement can be observed. The predicted results are calculated based on the assumption of constant floc size. At initial stage (<20 h), however, the floc size is small although the floc concentration is high. This results in the incomplete formation of floc. However, the constant floc size for over 20 h (i.e., corresponding stationary and endogenous phase) yields a good agreement between experimental and predicted results. In real activated sludge treatment processes, the aeration tank was always operated in a steady-state. In other words, the concentration and size of floc were not varied. Therefore, the population balance model to predict flotation efficiency will be widely applied for the determination of the operating conditions in the DAF process in water and wastewater treatments.

#### CONCLUSIONS

Experimental and theoretical studies of the DAF process were conducted for biological wastewater treatment. Contrary to our expectation, the removal efficiency of flocs corresponding in lag and exponential growth phases was lower, while that of flocs both in stationary and endogenous phases considerably increased. Thus, microbial flocs should be operated in stationary and endogenous phases. On the other hand, the value of initial adhesion efficiency was 0.3 for the lag and exponential growth phases and was a relatively higher value of 0.4 for the stationary and endogenous phases. The extended PB model developed in this study includes the entire range of Rey-

nolds number and also considers the effect of temperature. Good agreement between experimental and predicted flotation efficiency in the DAF process could be observed although there was a little discrepancy in lag and exponential growth phases. It was evident from our study that the DAF process is suitable as a secondary clarifier in an activated sludge process. The size of bubbles and flocs, the surface loading rate, and temperature highly affected the microbial flotation by the DAF process. In particular, the effect of temperature has to be taken into account in the DAF process because of the seasonal changes in Korea. Therefore, further study on the flotation efficiency will be systematically investigated by using the extended PB model incorporating the physical parameters (i.e., the water viscosity and the bubble density) as a function of temperature.

#### ACKNOWLEDGMENT

This work was supported by Grant No.R01-2004-000-11029-0 from the Korea Science & Engineering Foundation.

#### NOMENCLATURE

A	: 1st correlation parameter of water viscosity ( $=-2.471 \times 10$ )
a	: numerical constant [-]
B	: 2nd correlation parameter of water viscosity ( $=4.209 \times 10^3 \text{ K}$ )
C	: 3rd correlation parameter of water viscosity ( $=4.527 \times 10^{-2} \text{ K}^{-1}$ )
$C_D$	: drag coefficient [-]
c	: numerical constant for $i_{max}$ [-]
D	: 4th correlation parameter of water viscosity $-3.376 \times 10^{-5} \text{ [K}^{-2}\text{]}$
$d_{agglo}$	: diameter of bubble-floc agglomerate [m]
$d_b$	: diameter of bubble [m]
$d_p$	: diameter particle or floc [m]
F	: force [N]
g	: gravitational constant of acceleration ( $=9.80665 \text{ m/s}^2$ )
G	: turbulent intensity [ $\text{s}^{-1}$ ] ( $=(\varepsilon/\mu)^{1/2}$ )
$h_m$	: height of contact zone [m]
i	: number of bubbles attached on floc [-]
$i_{max}$	: maximum attachable number of bubbles on floc [-]
k	: collision rate constant [ $\text{m}^3/\text{s}$ ]
$M_{w,air}$	: molar mass of air bubble ( $=28.96 \text{ kg/kmol}$ )
$n_i$	: concentration of flocs with attached $i$ bubbles [ $\text{m}^{-3}$ ]
$n_{bubbles}$	: concentration of free bubble [ $\text{m}^{-3}$ ]
$N_0$	: initial concentration of floc [ $\text{m}^{-3}$ ]
$N_{Re}$	: Reynolds Number [-] ( $=\rho v_i d_{equiv}/\mu$ )
$P_{atm}$	: atmosphere pressure ( $=1.01325 \times 10^5 \text{ Pa}$ )
R	: gas constant ( $=8.3145 \times 10^3 \text{ Pa} \cdot \text{m}^3/\text{kmol} \cdot \text{K}$ )
t	: time [s]
$t_{contact}$	: retention time in contact zone [s]
T	: absolute Temperature [K]
$v_{i,cr}$	: critical rise velocity of bubble/floc agglomerate [m/s]
$v_i$	: rise velocity of bubble/floc agglomerate [m/s]
$v_{SL}$	: surface loading rate [m/s]

#### Greek Letters

$\alpha$	: adhesion efficiency [-]
$\varepsilon$	: turbulent dissipation of energy [ $\text{W/m}^3$ ]

$\phi$	: bubble volume concentration in contact zone [ $m^3/m^3$ ]
$\eta$	: removal or flotation efficiency [-]
$\kappa$	: dimensionless flotation rate constant [-]
$\mu$	: viscosity of water [ $kg/m \cdot s$ ]
$\rho$	: density of water [ $kg/m^3$ ]
$\rho_{agglom}$	: density of bubble/floc agglomerate [ $kg/m^3$ ]
$\rho_b$	: density of bubble [ $kg/m^3$ ]
$\rho_p$	: density of floc or particle [ $kg/m^3$ ]

### Superscripts and Subscripts

agglom	: agglomerate of bubble/floc
b	: air bubble
bubble	: bubbles
Buoyancy	: buoyancy
cr	: critical condition ( $N_{Re} \rightarrow 0$ )
Drag	: drag
i	: number of attached bubbles on floc
max	: maximum
0	: original or initial values
p	: particle or floc
*	: dimensionless variable

### Abbreviations

CGS	: conventional gravity sedimentation
COD	: chemical oxygen demand
DAF	: dissolved air flotation
PB	: population Balance
PBT	: population Balance in Transient
SS	: suspended solids

### REFERENCES

American Public Health Association, American Water Works Association and Water Pollution Control Federation (APHA-AWWA-WPCF), Standard methods for the examination of water and wastewater, 20th ed., Washington, DC (1998).

Bourgeois, J. C., Walsh, M. E. and Gagnon, G. A., "Treatment of drinking water residuals: comparing sedimentation and dissolved air flotation performance with optimal cation ratios," *Wat. Res.*, **38**, 1173 (2004).

Clift, R., Grace, J. R. and Weber, M. E., *Bubbles, drops, and particles*, Academic Press, New York (1978).

Edzwald, J. K., "Principles and applications of dissolved air flotation," *Wat. Sci. Tech.*, **31**(3-4), 1 (1995).

Fukushi, K., Tambo, N. and Matsui, Y., "A kinetic model for dissolved air flotation in water and wastewater treatment," *Wat. Sci. Tech.*, **31**(3-4), 37 (1995).

Kalinske, A. A. and Evans, R. R., *Comparison of flotation and sedimentation in treatment of industrial wastes*, Proceeding of Industrial Waste Conference 8th, pp. 64-71 (1953).

Kwak, D. H., Jung, H. J., Kim, S. J. and Lee, J. W., "Separation characteristics of inorganic particles from rainfalls in dissolved air flotation: A Korean perspective," *J. Sep. Tech.*, **40**, 3001 (2005).

Lee, J. E., Choi, W. S. and Lee, J. K., "A study of the bubble properties in the column flotation system," *Korean J. Chem. Eng.*, **20**, 942 (2003).

Lee, J. M., *Biochemical engineering*, Prentice-Hall, New Jersey, 2nd ed. (1992).

Lee, J. W., Jung, H. J., Kwak, D. H. and Chung, P. J., "Adsorption of dichloromethane from water onto a hydrophobic polymer resin XAD-1600," *Wat. Res.*, **39**, 617 (2005).

Lee, J. W., Yang, T. H., Jung, H. J., Kim, S. J. and Kwak, D. H., "Flotation efficiency of powdered activated carbon in dissolved air flotation process," *Wat. Res.* (under review, 2005).

Lee, M. G and Hano, T., "Effects of hourly load variation on treatment characteristics in anaerobic-aerobic activated sludge process," *Korean J. Chem. Eng.*, **18**, 178 (2001).

Leppinen, D. M., Dalziel, S. B. and Linden, P. F., "Modeling the global efficiency of dissolved air flotation," *Wat. Sci. Tech.*, **43**(8), 159 (2001).

Leppinen, D. M. and Dalziel, S. B., "Bubble size distribution in dissolved air flotation tanks," *J. Wat. Suppl: Res. & Tech.-AQUA*, **53**(8), 531 (2004).

Liers, S., Baeyens, J. and Mochtar, I., "Modeling dissolved air flotation," *Water Environ. Res.*, **68**(6), 1061 (1996).

Matsui, Y., Fukushi, K. and Tambo, N., "Modeling, simulation and operation parameters of dissolved air flotation," *J. Wat. Suppl: Res. & Tech.-AQUA*, **47**, 9 (1998).

Martins, A. M. P., Pagilla, K., Heijnen, J. J. and Loosdrecht, M. C. M., "Filamentous bulking sludge - a critical review," *Wat. Res.*, **38**, 793 (2004).

Reid, R. C., Prausnitz, J. M. and Poling, B. E., *The properties of gases and liquids*, McGraw-Hill, 4th ed. (1987).

Rodrigues, R. T. and Rubio, J., "New basis for measuring the size distribution of bubbles," *Min. Eng.*, **16**, 757 (2003).

Tambo, N. and Fukushi, K., "A kinetic study of dissolved air flotation," *J. JWWA*, **60**, 22 (1985).

Tambo, N., Fukushi, K. and Matsui, Y., "An analysis of air bubble attachment process of dissolved air flotation," *J. JWWA*, **61**, 2 (1985).

Vlyssides, A. G., Mai, S. T. and Barampouti, E. M., "Bubble size distribution formed by depressurizing air-saturated water," *Ind. Eng. Chem. Res.*, **43**, 2775 (2004).

Zabel, T., "The advantages of dissolved-air flotation for water treatment," *J. AWWA*, **77**(5), 42 (1985).